Peer-reviewed version available at *Materials* **2017**, *10*, 147; doi:10.3390/ma10020147

*Article*

# Band Gap Tuning in 2D Layered Materials by Angular Rotation

**Javier Polanco-González [1], Jesús Alfredo Carranco-Rodríguez [2], José Luis Enríquez-Carrejo [1], Pierre Giovanni Mani-González [1], José Manuel Domínguez-Esquivel [3] and Manuel Ramos [1],***

[1] Departamento de Física y Matemáticas, Instituto de Ingeniería y Tecnología, Universidad Autónoma de Cd. Juárez, Avenida del Charro #450 N. Cd. Juárez, Chihuahua C.P. 32310, México; javier.polanco@uacj.mx (J.P.-G.); jose.enriquez@uacj.mx (J.L.E.-C.); pierre.mani@uacj.mx (P.G.M.-G.)

[2] Materials Science and Engineering, McMaster University, 1280 Main St. West, Hamilton, ON L8S 4L7, Canada; carrancj@mcmaster.ca

[3] Instituto Mexicano del Petróleo, Eje Central Lázaro Cárdenas No 152, México D.F. 07730, México; jmdoming@imp.mx

* Correspondence: manuel.ramos@uacj.mx; Tel.: +52-656-688-6909; Fax: +52-656-688-4813

**Abstract:** We present a series of computer-assisted high resolution transmission electron (HRTEM) simulations to determine Moiré patters by induced twisting effects between slabs at rotational angles of 3°, 5°, 8°, and 16°, for molybdenum disulfide, graphene, tungsten disulfide, and tungsten selenide layered materials. In order to investigate the electronic structure, a series of numerical simulations using DFT methods was completed using CASTEP with a generalized gradient approximation to determine both band structure and density of states on honeycomb like new superlattices. Our results indicate metallic transitions when rotation approaches 8° with respect to each other for most of the two-dimensional systems that were analyzed.

**Keywords:** Moiré patterns; $MoS_2$; Graphene; $WS_2$; $WSe_2$; HRTEM

## 1. Introduction

Layered materials have attracted much attention lately, because of its exceptional catalytic, photovoltaic and semiconducting properties [1, 2]. An extensive characterization for 2*D* materials like molybdenum disulfide ($MoS_2$), tungsten disulfide ($WS_2$), tungsten diselenide ($WSe_2$) and graphene has occurred in past decades, using field emission gun microscopic techniques, such as scanning electron [3], transmission electron [4] and tunneling microscopy [5] with high accuracy. Observations reveal in detail their layered sandwich structure consisting of S-Mo(W)-S and Se-W-Se layers held together at a distance of 0.62 nm by weak Van der Waals forces [6]. The formation of Moiré patterns in those particular layered materials was observed by Kobayashi using scanning tunneling microscopy [5], and by Yacaman implementing transmission electron microscopy technique [7], both concluding that formation of Moiré patterns is attributed to strain effects between layered slabs with respect to the [001] crystallographic direction, creating honeycomb like structures. Additionally, Jasinski observed similar Moiré patterns for single layers of graphene attributed to a 5° of rotation between slabs [8]. Recently, we were able to determine the electronic band structure of strained 2R-$MoS_2$ (SG-R3m) when is rotated about 10° (with respect to (001)-basal plane). Our density functional theory (DFT) calculations determined a rapid semiconducting to metallic state transitions, as indicated by two irreducible points near K→Γ and A→ L points when sampling over Brillouin zone with Fermi wave vector values of $\boldsymbol{k_F}$ at ~ 0.47 Å-1 and $\boldsymbol{k_F}$ ~ 0.37 Å-1 near 10° to 12° of rotation [9]. However, the point we would like to introduce in here is the formation of a new lattice parameter, which is a new O-lattice formed by rotation of crystallographic structures as described by Bollman in late 70´s [10] and presented by Remskar [11] and Gomez and Romeu for the reciprocal lattice rotation between two crystals [12]. Creating this natural strain between slabs is relatively easy due to its weak Van der Waals bonding between slabs, and the reason of why it was possible to create a single layer of graphene as presented by Geim and Novoselov et al. [13]. Zhang et al. were able to achieve tuning of single layers of graphene band gap when fabricating a field-effect transistor [14], thus we present in here a series of new O-lattices for honeycomb-like structures as formed by rotating 2*D* layered structures with respect to (001) basal plane, along with a series of computer assisted electronic structure calculations using density functional methods to identify if there is any transition (tuning) from semiconducting to metallic and vice versa on those specific nanostructure materials.

## 2. Results and Discussion

Typical Moiré patterns are observed when two 2*D* lattices are rotated at a certain angle, and observation is made directly at their basal plane, usually called (001), over c-axis direction. We had reported previously those observations in both experimental HRTEM and simulated for 2R-$MoS_2$ slabs when rotated about $12^{\circ}$ in c-direction [3,9]. Furthermore, we were able to produce formation of Moiré patterns on other materials (i.e. tungsten disulfide ($WS_2$), graphene and tungsten diselenide ($WSe_2$)) by achieving this lattice rotation on the molecular models, which creates honeycomb-like features, observing as well the formation of new O-lattices as presented in Figure 1 (*corresponding to distance between ending points at edge of honeycomb-like*). Later, those molecular models were subjected to HRTEM simulations varying ***a, b*** coefficients in the projected potential as described by equation 1 in section 3.1. The as-simulated sequence of images are presented in figures 2, 3, 4 and 5; it is possible to determine the formation of large O-lattice with non-defined honey-comb structure for angles of rotation corresponding to 3° and strong honey-comb structure at 16°, moreover the resulting O-lattice was measured digitally using BIOVIA® Materials Studio crystal builder tool, our findings are presented (*for easy reading*) in table 1 and graphically by the inset of red arrows in figure 1.

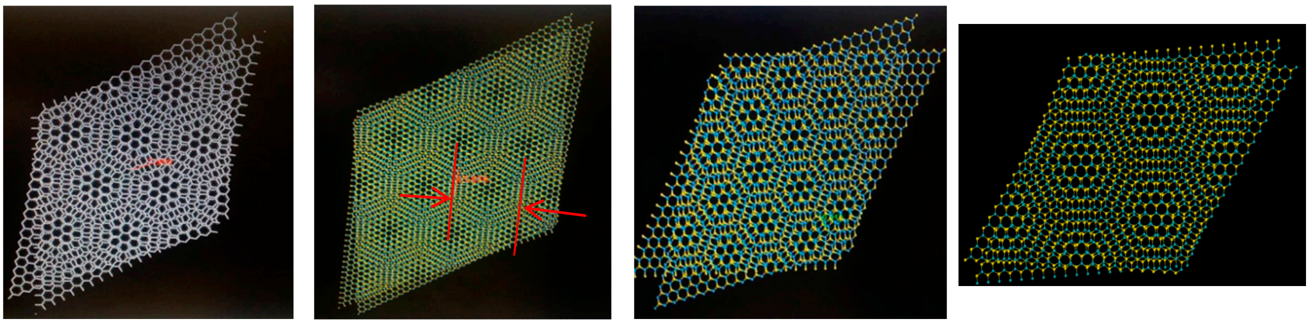

Figure 1.- Moiré pattern as formed by angular rotation of 2*D* layered materials molecular models. From left to right: graphene, tungsten diselenide ($WSe_2$), tungsten disulfide ($WS_2$) and molybdenum disulfide ($MoS_2$) at 19° of rotation.

It is important to mention that Moire patterns are not typically seen by HRTEM techniques for bulk 2*D*-layered materials, for example when surveying 2R-$MoS_2$ slabs, fringes like is commonly observed and it is possible to determine the Van der Waals forces gap of 6.2 Å between slabs [18], and also to see clearly that synthesis conditions can cause "turbostraticity" bending of layered structure, thus one must have cautious procedures when fabricating nanoscale-organized devices [19]. Therefore, analysis of the electronic structure corresponding to rotated 2*D*-layered structures needs to be performed. The electronic structure of these O-lattices as calculated by DFT methods, reflect a rapid transition for the majority of those layered structures, our findings are presented in figure 3.

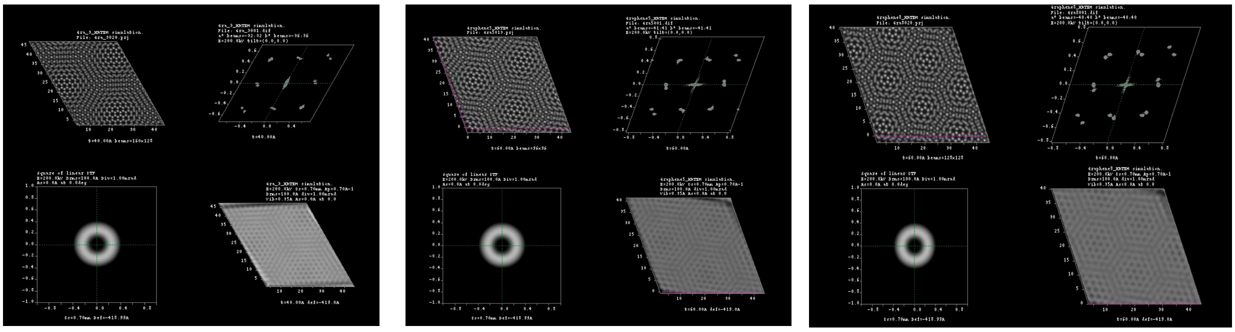

**Figure 2**.- HRTEM simulation for 3°, 8° and 16° of rotation in graphene molecular structure.

Peer-reviewed version available at *Materials* **2017**, *10*, 147; doi:10.3390/ma10020147

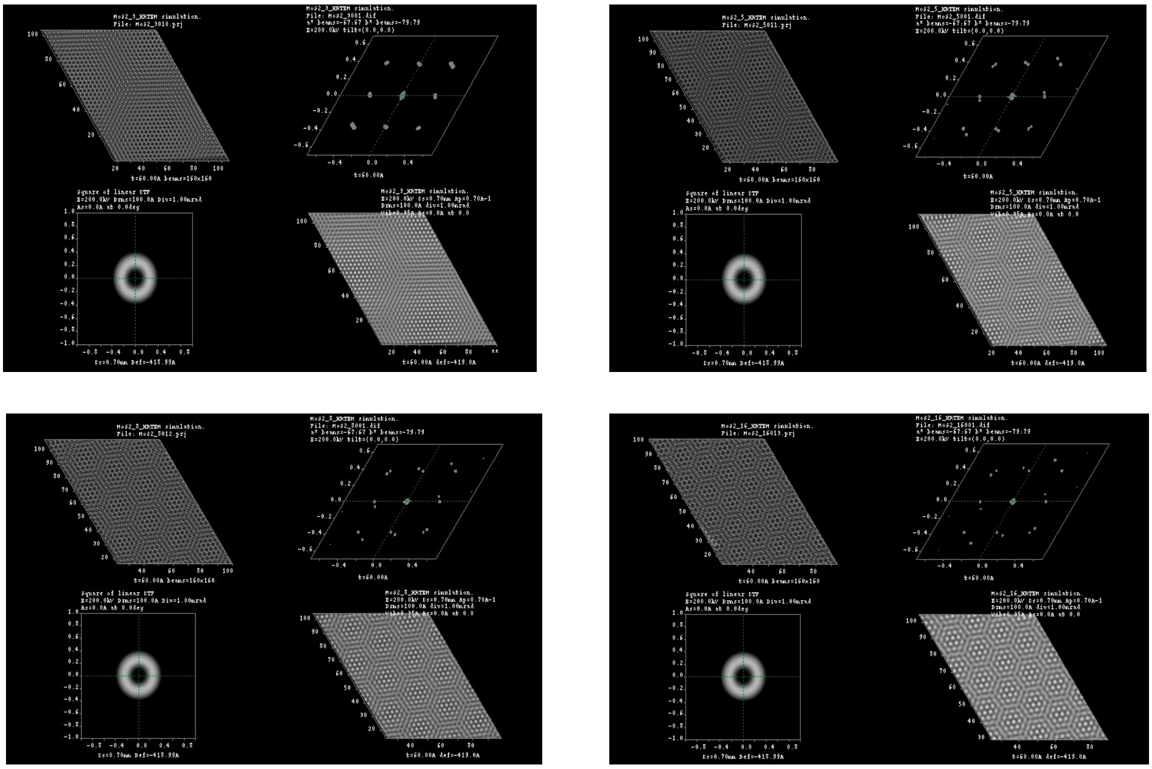

**Figure 3.-** HRTEM simulation for 3°, 5°, 8° and 16° of rotation in molybdenum disulfide molecular structure.

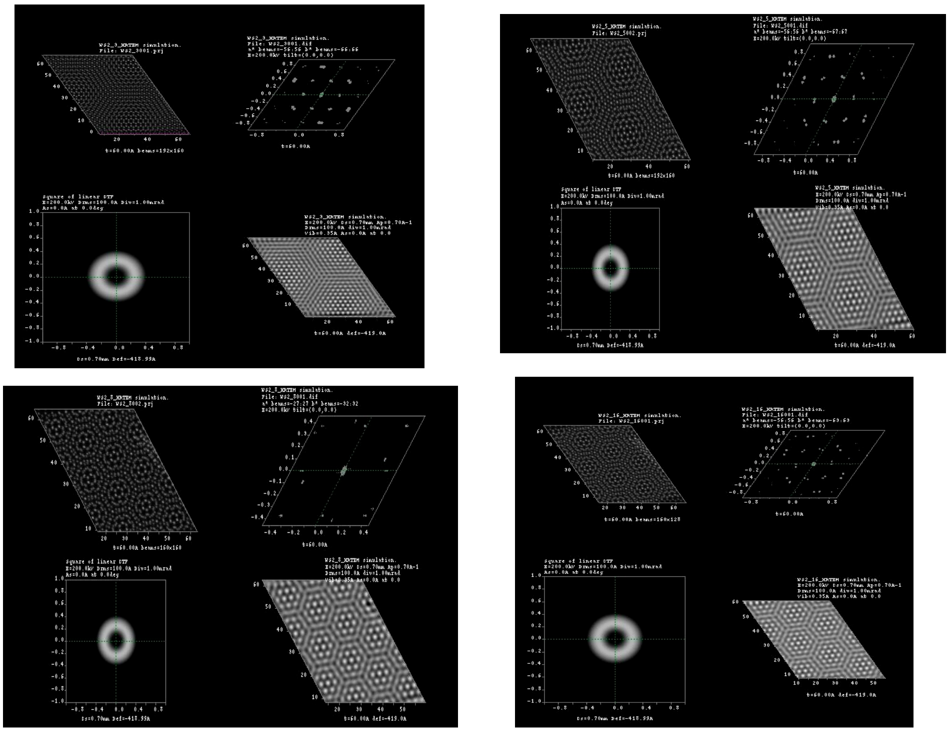

**Figure 4.-** HRTEM simulation for 3°, 5°, 8° and 16° of rotation in tungsten disulfide molecular structure.

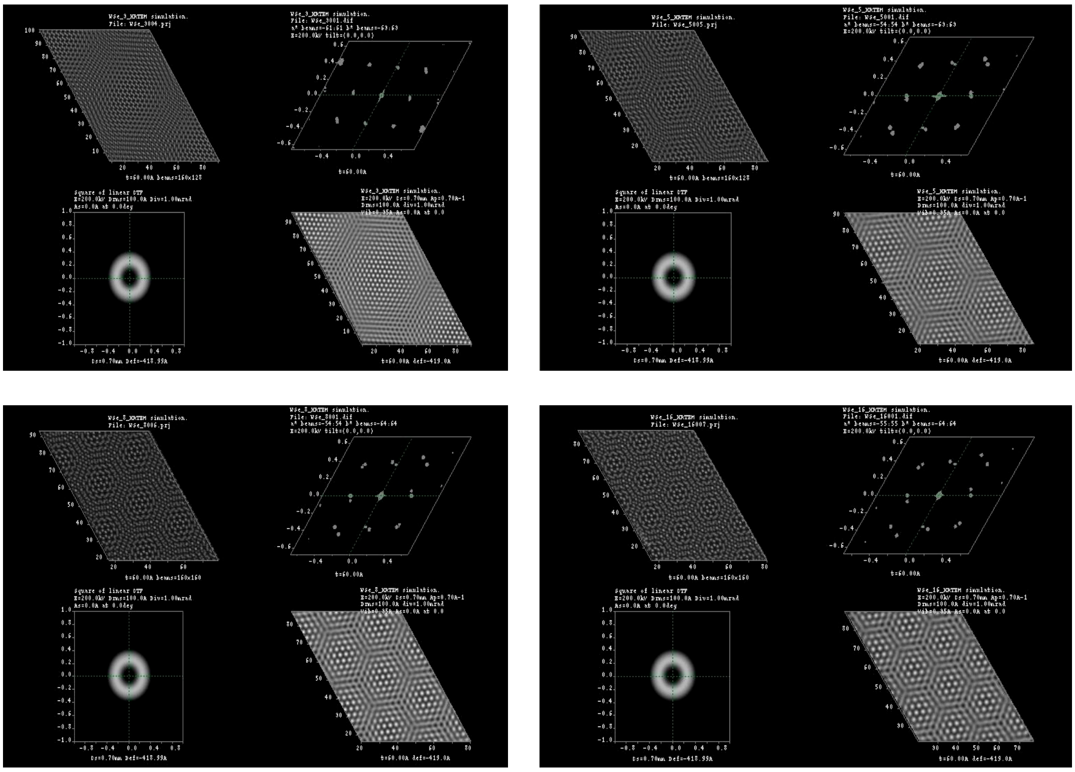

**Figure 5.**- HRTEM simulation for 3°, 5°, 8° and 16° of rotation in tungsten diselenide molecular structure.

| Rotation Angle | Graphene | $MoS_2$ | WSe | $WS_2$ |
|---|---|---|---|---|
| **3°** | 12.300 Å | 25.328 Å | 22.974 Å | 18.948 Å |
| **5°** | 9.840 Å | 15.830 Å | 19.692 Å | 15.796 Å |
| **8°** | 8.639 Å | 15.736 Å | 14.899 Å | 9.950 Å |
| **16°** | 7.380 Å | 12.725 Å | 9.846 Å | 9.474 Å |

**Table 1**.- O-lattice distribution for 2D layered materials corresponding to molecular structures at various rotation angles.

In order to determine the electronic structure of those new O-lattices as created by angular rotation of molecular structures, we proceed with band structure using CASTEP as described in section 3.2 and elsewhere [9], our results indicate some transitions from metallic into a wide band gap semiconductor for the graphene layers as presented by Band Structure and Density of States corresponding to 0° and 16° shown in figure 6. The opposite occurs for the case of $WS_2$ and WSe as well as presented for $MoS_2$ (presented in ref. 9) molecular structures, as presented in figure 7 and 8.

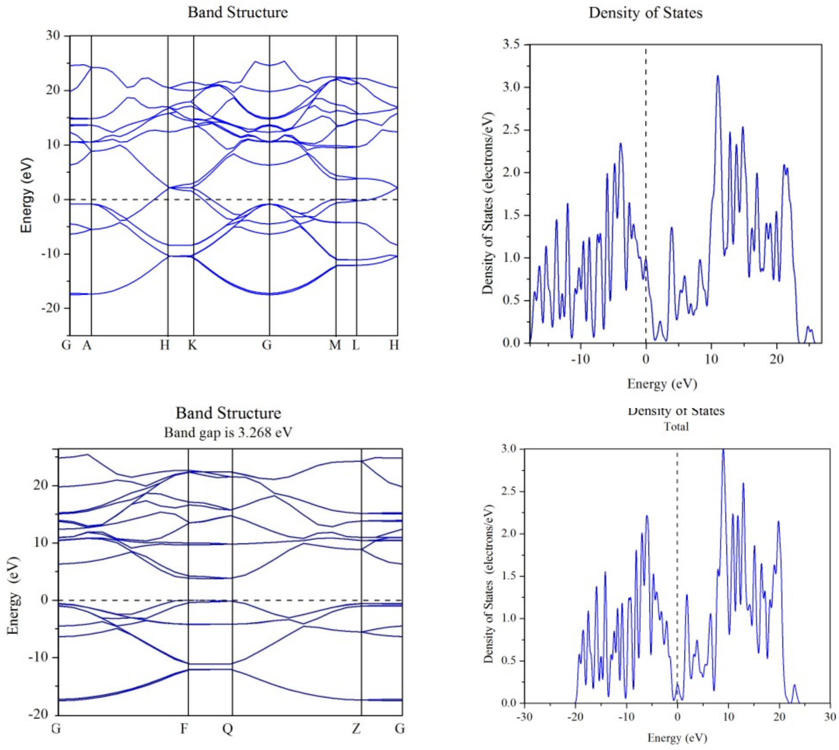

**Figure 6.**- Band structure and density of states plots corresponding to 0°(top) and 16° (bottom) of rotation in graphene molecular structure, a tuning on the electronic band gap is observed.

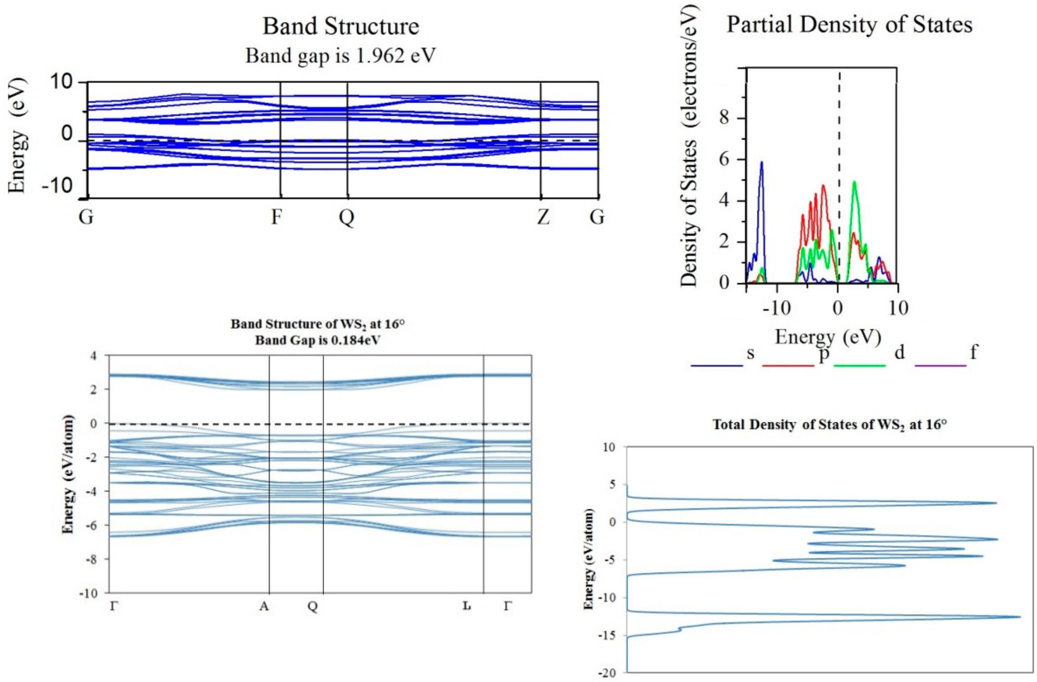

**Figure 7.**- Band structure and partial-total density of states plots corresponding to 0°(top) and 16° (bottom) of rotation in WS$_2$ molecular structure.

Peer-reviewed version available at *Materials* **2017**, *10*, 147; doi:10.3390/ma10020147

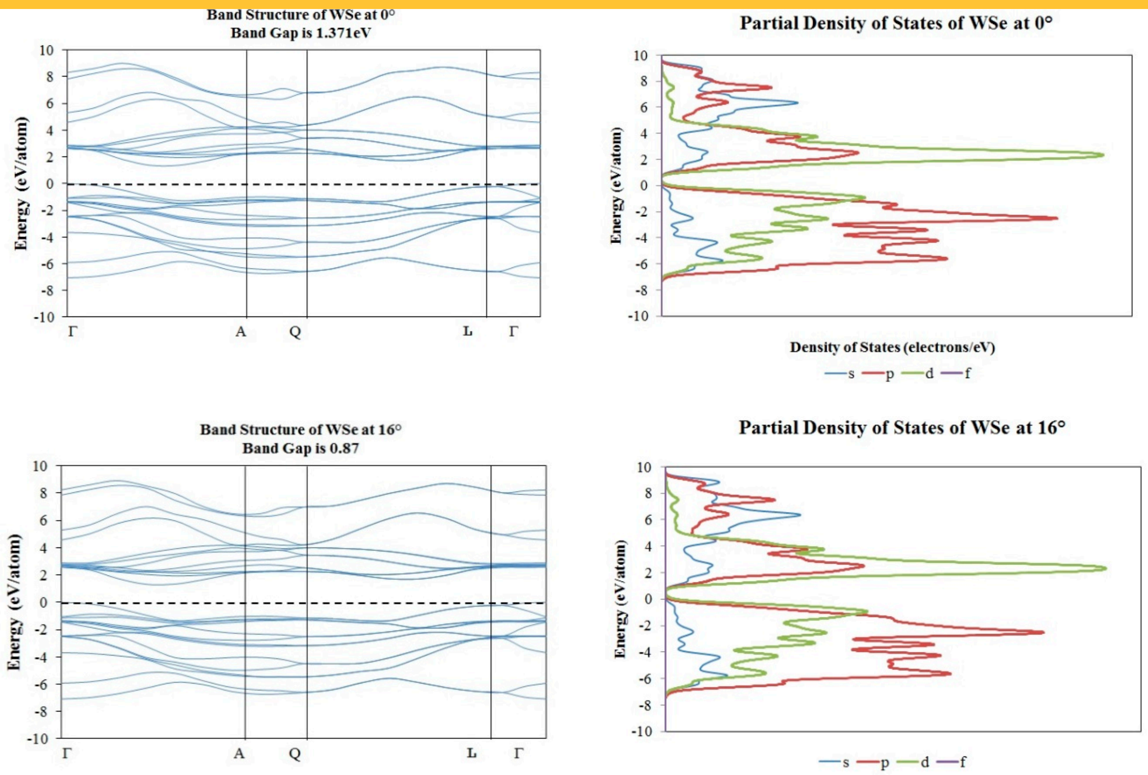

**Figure 8.-** Band structure and partial density of states plots corresponding to 0°(top) and 16°(bottom) of rotation in WSe molecular structure.

Because of the large data calculations, added all band gaps values as plotted with degree of rotation, as presented in figure 9. One can conclude that using this fast and low cost approach to understand both Bollman O-lattices formation due to "twisting" of two layered molecular structures, subjected to numerical density functional theory computations. Since, it is possible achieve with high accuracy as reported before [9] a high throughput approximation by using CASTEP algorithm to describe electronic structure transitions in layered molecular nanostructure materials.

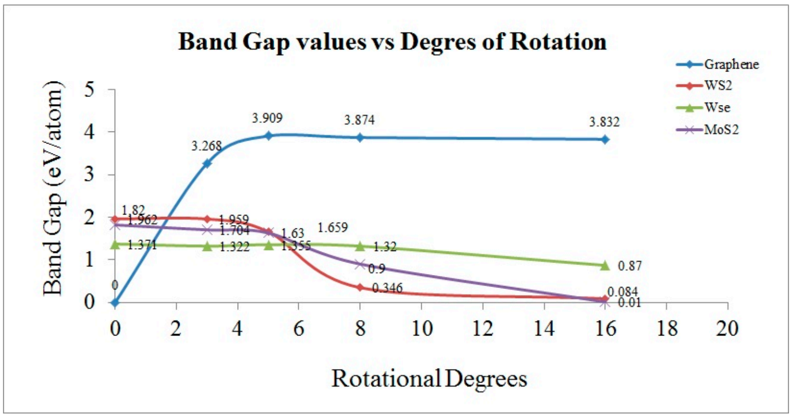

**Figure 9.-** Band gap values of layered molecular models corresponding to graphene, $WS_2$, WSe and $MoS_2$, as obtained from DFT numerical simulations using CASTEP algorithm.

Peer-reviewed version available at *Materials* **2017**, *10*, 147; doi:10.3390/ma10020147

## 3. Computational Details

### *3.1 Multislice HRTEM Simulations*

Computer assisted transmission electron microscope simulations were completed using a fully dynamical calculation multi-slice method using projected potential:

$$f(U)=\sum_{i=1}^{n}a_i e^{(-ibU^2)} \qquad (1)$$

Where $U$ represents the coordinates in reciprocal space (u, v, w) as described by Gomez-Rodríguez [15], projecting the potential over (001) c-axis and adjusting $a$ and $b$ coefficients in a range of $98 < a < 128$ and $96 < b < 128$ to obtain the optimum conditions in comparison with some experimental HRTEM results, as presented in the literature [3,7]. The crystallographic structures were built using graphical user interface as presented in builder module of Accelrys 6.1-Materials Studio® package with crystallographic parameters as found from JCPDS cards. All honeycomb structures were created when exerting mechanical rotation at 3°, 5°, 8°, and 16°, with respect to the (001) *c*-basal axis; keeping always an inter-layer distance of 6.20 Å from molybdenum to molybdenum (Mo-Mo) in $MoS_2$, 6.4 Å from tungsten to tungsten (W-W) in $WS_2$ and 6.7 Å in $WSe_2$ and 3.4Å in carbon to carbon as found in carbonic rings of graphene layers.

### *3.2. Density Functional Theory Calculations*

The electronic structure of each strain O-lattice was calculated using a seed from two large layers were as built in Materials Studio 6.1 graphical user interface, each superlattice (O-lattice) consisted of 1804 atoms approximately, as shown on figure 1. Thus, to achieve fast conversion criteria and to reduce computational time, the electronic calculations were performed using a representative portion called here "seed", consisting of 12 to 24 atoms, as shown on inset of figure 1. The "seed", was placed in a P1 (no symmetry) crystal and with varying lattice parameters from $16.0\ \text{Å} \leq a \leq 18.0\ \text{Å}$, $17.0\ \text{Å} \leq b \leq 21.0\ \text{Å}$, $15.0 \leq c \leq 17.0\ \text{Å}$ and crystal lattice angles of $\alpha = \beta = 90^{\circ}$ and $\gamma = 120^{\circ}$. These particular distances were selected cautiously to avoid interaction with neighboring atoms in periodic cells conditions, which could yield incorrect results in both band structure and density of states calculations. Before calculating the density of states and band structure calculations, both untwisted and twisted "seeds" were subjected to geometrical optimizations using the Broyden–Fletcher–Goldfarb–Shanno algorithm, as described by Fischer and Almlöf [16]. All DFT computations were performed using Cambridge Serial Total Energy Package (CASTEP) with a revised Perdew-Burke-Ernzerhof functional [17], general gradient approximation, cutoff energy of 300 eV in the reciprocal space for gamma point only with a self-consistent field (SCF) convergence threshold of $1 \times 10^{-6}$ eV per atom and without any thermal smearing.

## 4. Conclusions

From previous investigations it is possible to achieve observations of $MoS_2$ stacked structure using experimental HRTEM, then using dynamical multi-slice HRTEM simulations it was possible to determine a structural meaning of those honeycomb observations. In here, we present a more extensive study including graphene, $WS_2$ and $WSe_2$ layered materials, observing a new concept as presented by

Peer-reviewed version available at *Materials* **2017**, *10*, 147; doi:10.3390/ma10020147

Bollman corresponding to formation of new lattice, so-called O-lattice. To further understand the electronic structure nature of this new O-lattice, we proceeded with DFT numerical simulations where it was possible to determine some transitions and band gap reduction due to strain caused by rotating the lattices as presented in here. Finally, we conclude this low cost computational approach allows us to understand the nature of these "honeycomb-like" new O-lattices.

## Acknowledgments

Instituto de Ingeniería y Tecnología de Universidad Autónoma de Cd. Juárez and University of Texas at El Paso for usage of computational resources. Javier Polanco-Gonzalez thank the Consejo Nacional de Ciencia y Tecnología (CONACyT-México) for financial support on repatriation fellowship #262748.

## Author Contributions

Javier Polanco-Gonzalez and J. Alfredo Carranco-Rodríguez were in charge of computer assisted numerical simulations by DFT methods. Manuel Ramos was in charge of computer assisted transmission electron images. Pierre G. Mani-Gonzalez and Jose L. Enríquez-Carrejo were in charge of data processing and interpretation. Manuscript was completed and written by M. Ramos, J.L. Enríquez-C and J. Polanco-G.

## *Conflicts of Interest

The authors declare no conflict of interest.

## References

1.- O. Weisser, S. Landa, Pergamon Press, N.Y. (1973).
2.- Néstor Perea-López, Zhong Lin, Nihar R Pradhan, Agustín Iñiguez-Rábago, Ana Laura Elías, Amber McCreary, Jun Lou, Pulickel M. Ajayan, Humberto Terrones, Luis Balicas and Mauricio Terrones, 2D Materials, 1 (2014).
3.- Russell R. Chianelli, Albert F. Ruppert, Miguel José-Yacamán, Armando Váquez-Zavala, Catalysis Today, 23, (1995).
4.- A. Vazquez, Materials Letters, 35 (1998) 22-27.
5.- Katsuyoshi Kobayashi, J. Vac. Sci. Technol. B 14(2), (1996).
6.- F. Jellinek, G. Brauer, H. Müller, Nature 185 (1960) 376-377.
7.- J. Reyes-Gasga, S. Tehuacanero and M. José-Yacamán, Microscopy Research and Technique, 40:2–9, (1998).
8.- J. B. Jasinski, S. Dumpala, G. U. Sumanasekera, M. K. Sunkara, and P. J. Ouseph, Applied Physics Lettters, 99, 073104 (2011).
9.- Manuel A. Ramos, Russell Chianelli, Jose Luis Enriquez-Carrejo, Gabriel A. Gonzalez and Gilles Berhault, Computational Materials Science 84 (2014) 18–22.
10.- W. Bollman, Crysrtal defects and crystalline interfaces, Springer-Verlag, Berlin (1970) ISBN :

978-3-642-49173-3 (e-book).

11.- M. Remskar, A. Mrzel, Z. Skraba, A. Jesih, M. Ceh, J. Demšar, P. Stadelmann, F. Lévy, D. Mihailovic, Science 292 (2001) 479-481.

12.- A. Gómez Rodríguez and D. Romeu Casajuana, Revista Mexicana de Física, 53 (2) 139–143, (2007).

13.- K. S. Novoselov, A.K. Geim, S.V. Morozov, D. Jiang, Y. Zhang, S.V. Dubonos, I.V.Grigorieva, A.A. Firsov. Science 306 (2004) 666–669.

14.- Yuanbo Zhang, Tsung-Ta Tang, Caglar Girit, Zhao Hao, Michael C. Martin, Alex Zettl, Michael F. Crommie, Y. Ron Shen & Feng Wang, Nature Letters, Vol 459, (2009).

15.- A. Gómez-Rodríguez, L.M. Beltrán-del-Río, R. Herrera-Becerra, Ultramicroscopy 110 (2010) 95-104.

16.- T. H. Fischer, J. Almlöf, J. Phys. Chem. 96 (1992) 9768-9774.

17.- J. P. Perdew, K. Burke, and M. Ernzerhof, Phys. Rev. Lett. 77, 3865 (1996).